

## Introduction

Co-located sites of the space-geodetic techniques GPS and VLBI allow for a comparison of the common parameters determined by these two independent techniques. Long-time series of homogeneously reprocessed GPS and VLBI data computed by TU Munich/TU Dresden (GPS) and DGFI (VLBI) covering the time interval from 1994 till 2005 provide the basis for our comparisons of different troposphere mapping functions and hydrostatic a priori delays. In order to minimize systematic effects due to differences in modeling and parameterization of the GPS and VLBI solutions, all important models as well as the parameterization of the software packages Bernese and OCCAM used for the GPS and VLBI processing have been harmonized. Thus, a maximum level of consistency is guaranteed.

## Troposphere Modeling

The troposphere slant delay  $\Delta q_{trp}$  is expressed by

$$\Delta q_{trp}(z_R^S, A_R^S) = f_{apr}(z_R^S) \Delta q_{apr} + f_{est}(z_R^S) \Delta q_{est} + \Delta q_n \frac{\partial f_{est}}{\partial z} \cos(A_R^S) + \Delta q_e \frac{\partial f_{est}}{\partial z} \sin(A_R^S) \quad (1)$$

with

$z_R^S$	zenith distance of satellite/quasar $S$ observed by receiver/telescope $R$
$A_R^S$	azimuth of satellite/quasar $S$ observed by receiver/telescope $R$
$f_{apr}(z_R^S)$	hydrostatic mapping function
$\Delta q_{apr}$	hydrostatic (a priori) troposphere zenith delay
$f_{est}(z_R^S)$	wet mapping function
$\Delta q_{est}$	estimated (wet) troposphere zenith delay
$\Delta q_n$	troposphere gradient in north-south direction
$\Delta q_e$	troposphere gradient in east-west direction

$\Delta q_{apr} + \Delta q_{est}$  is referred to as zenith total delay (ZTD). As the troposphere mapping functions have a significant influence on the estimated troposphere parameters and station coordinates, we computed five GPS and VLBI solutions, respectively, that only differ in the mapping functions and the a priori hydrostatic delays. The following mapping functions have been used:

- Niell Mapping Function (NMF), *Niell (1996)*
- Global Mapping Function (GMF), *Boehm et al. (2006a)*
- Isobaric Mapping Function (IMF), *Niell (2000)*
- Vienna Mapping Function 1 (VMF1), *Boehm et al. (2006b)*

For the hydrostatic a priori delays, two different approaches have been used

- Hydrostatic delays computed with the standard atmosphere of *Berg (1948)* and the *Saastamoinen (1973)* model
- Hydrostatic delays derived from numerical weather model data (ECMWF) provided by TU Vienna (<http://mars.hg.tuwien.ac.at/~ecmwf1/>)

The different GPS and VLBI solutions are listed in Table 1.

Solution	hydrostatic mapping function	wet mapping function	hydrostatic a priori delay
NMF	hydrostatic NMF	wet NMF	Berg/Saastamoinen
GMF	hydrostatic GMF	wet GMF	Berg/Saastamoinen
IMF	hydrostatic IMF	wet NMF	Berg/Saastamoinen
VMF1 const	hydrostatic VMF1	wet VMF1	Berg/Saastamoinen
VMF1 ECMWF	hydrostatic VMF1	wet VMF1	ECMWF

TABLE 1: GPS and VLBI solutions with different mapping functions and hydrostatic a priori delays.

## GPS and VLBI Processing

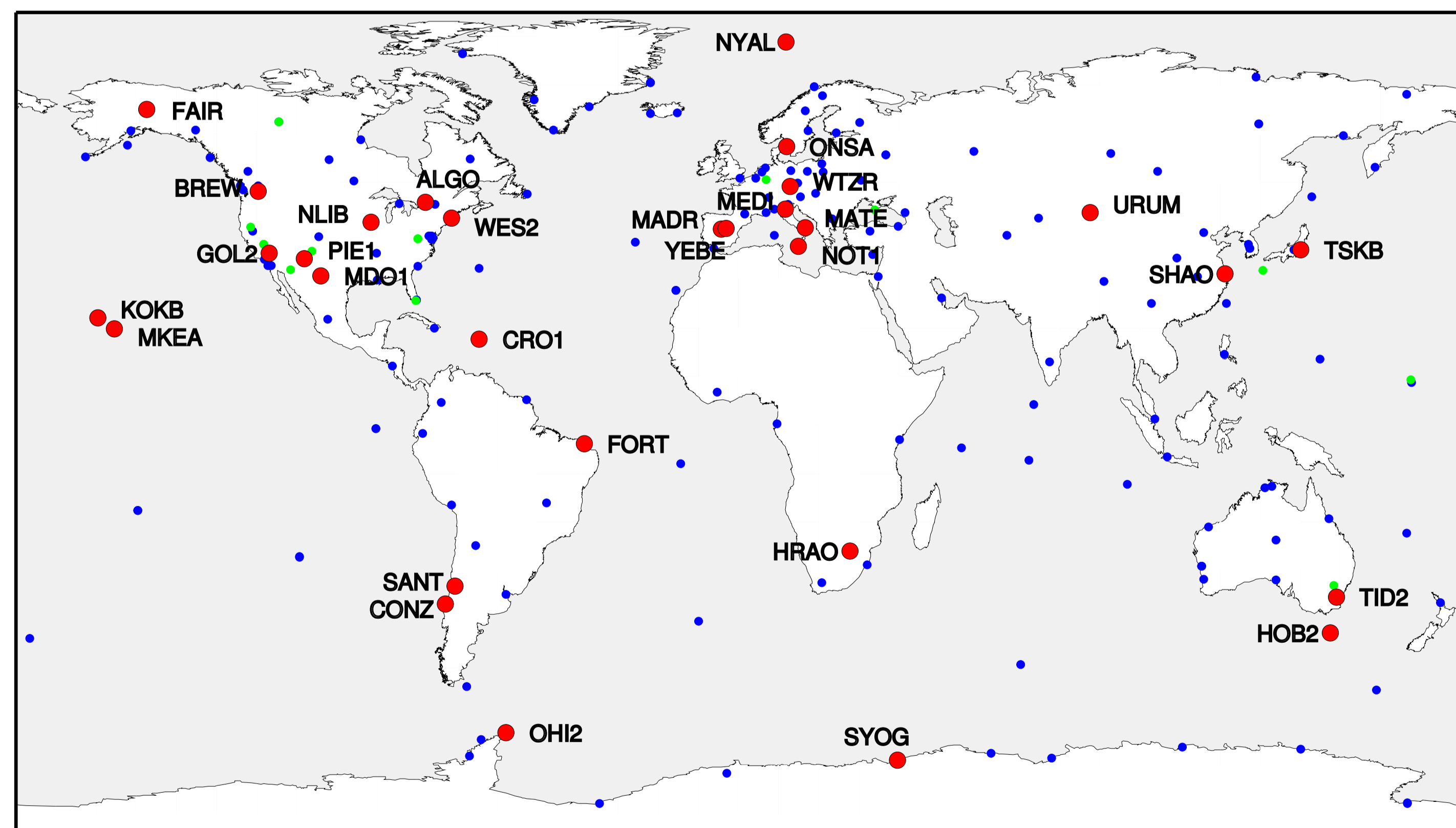


FIGURE 1: Co-located GPS and VLBI stations. If more than one GPS site is located at a station, only the name of the primary GPS site is given.

The GPS solutions are based on the complete and homogeneous reprocessing of a global GPS network conducted by TU Dresden and TU Munich (*Steigenberger et al., 2006*) using a modified version of the Bernese GPS Software 5.0. The results of 1-day solutions covering the time period from 1 January 1994 till 30 October 2005 are used here. Elevation-dependent weighting and a cut-off angle of  $3^\circ$  were applied. The VLBI solutions are based on observations of 49 telescopes from 2760 24-hour sessions between 4 January 1984 and 30 December 2005 using OCCAM 6.1 (*Titov et al., 2004*) and DOGS-CS (*Angermann et al., 2004*). The terrestrial and the celestial reference frame as well as the ERPs were estimated simultaneously to guarantee full consistency within the VLBI solution (*Tesmer et al., 2004*). An elevation cut-off angle of  $5^\circ$  and a refined stochastic model that mainly consists of an elevation-dependent weighting (*Tesmer and Kutterer, 2004*) were applied.

Figure 1 shows the GPS and VLBI tracking networks. Important characteristics of the GPS and the VLBI solutions are summarized in Table 2.

	GPS	VLBI
Software	Bernese 5.0	OCCAM 6.1, DOGS-CS
Data	4322 1-day solutions (1994-2005)	2760 24-hour sessions (1984-2005)
Number of stations	202 (40-160 per day)	49 (3 to 20 per session)
Datum	NNR w.r.t. IGB00	NNR/NTT w.r.t. ITRF2000
Solution type	global solution including station coordinates and ERPs	simultaneous estimation of TRF, CRF and ERPs
Troposphere zenith delays	2-hour resolution	1-hour resolution

TABLE 2: Important characteristics of the GPS and VLBI solutions.

## Results

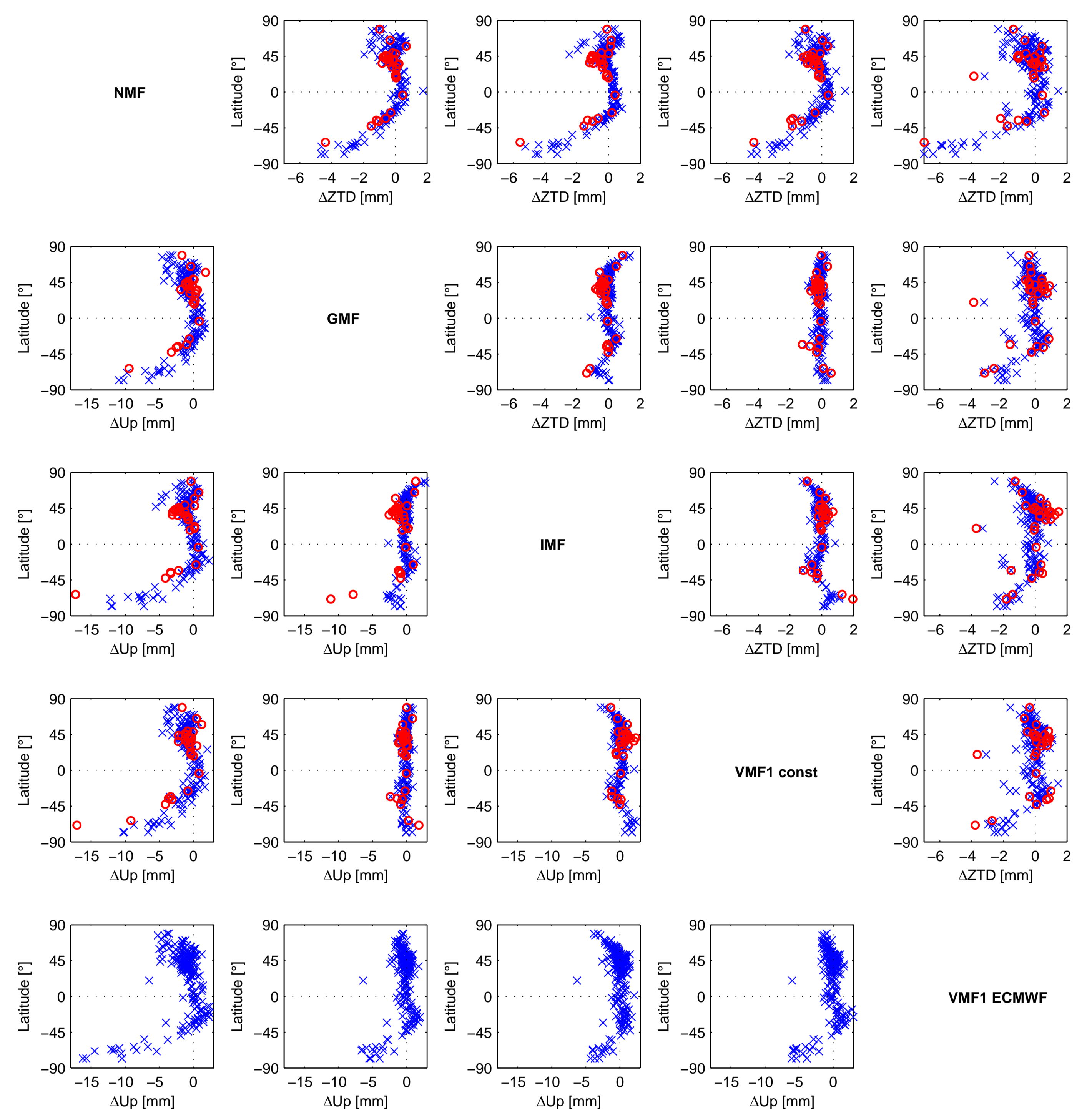


FIGURE 2: Station height and zenith total delay differences between all solutions listed in Table 1. The lower triangle shows the station height differences, the upper triangle the zenith total delay differences. The differences refer to the solution IDs given on the diagonal (e.g., the lowest plot on the left hand side shows the coordinate differences between solutions NMF and VMF1 ECMWF). GPS-derived differences are given in blue, VLBI-derived differences in red (VLBI coordinates not available for solution VMF1 ECMWF).

Figure 2 shows the station height and troposphere zenith total delay differences of all solutions listed in Table 1. All comparisons with NMF show a clear latitude-dependent systematic pattern due to the deficiencies of the NMF:

- the seasonal behavior of the southern and the northern hemisphere is the same (phase difference of  $180^\circ$ )
- the equatorial region from  $15^\circ\text{S}$  to  $15^\circ\text{N}$  is described by the  $15^\circ\text{N}$  latitude profile
- the polar regions with latitudes larger than  $75^\circ$  are described by the  $75^\circ\text{N}$  latitude profile

In particular the station height differences of more than 1 cm and the ZTD differences of up to 7 mm in Antarctica are striking. But also in the northern hemisphere there is a slightly latitude-dependent pattern visible.

IMF also shows a slight latitude-dependent systematics compared to GMF and VMF1 although this effect is much smaller compared to NMF. On the other hand, there is no systematic pattern in the comparisons of GMF and VMF1 visible. This is what we would have expected, as the GMF and the VMF1 were generated in a consistent way.

By comparing solution VMF1 const with solution VMF1 ECMWF the influence of different hydrostatic a priori delays can be studied. Again, the largest differences (more than 5 mm in the station height and more than 3 mm in the ZTD) occur in Antarctica due to the deficiencies of the standard atmosphere applied for solution VMF1 const.

## References

- Angermann, D., H. Drewes, M. Krügel, B. Meisel, M. Gerstl, R. Kelm, H. Müller, W. Seemüller, and V. Tesmer (2004), ITRS combination center at DGFI - a terrestrial reference frame realization 2003, München.
- Berg, H. (1948), *Allgemeine Meteorologie*, Dümmlers Verlag, Bonn.
- Boehm, J., A. Niell, P. Tregoning, and H. Schuh (2006a), Global mapping function (GMF): A new empirical mapping function based on numerical weather model data, *Geophysical Research Letters*, 33, L07304, doi:10.1029/2005GL025546.
- Boehm, J., B. Werl, and H. Schuh (2006b), Troposphere mapping functions for GPS and very long baseline interferometry from European Centre for Medium-Range Weather Forecasts operational analysis data, *Journal of Geophysical Research*, 111, B02406, doi:10.1029/2005JG003629.
- Niell, A. (1996), Global mapping functions for the atmosphere delay at radio wavelengths, *Journal of Geophysical Research*, 101(B2), 3227-3246.
- Niell, A. (2000), Improved atmospheric mapping functions for VLBI and GPS, *Earth Planets Space*, 52, 699-702.
- Saastamoinen, J. (1973), Contributions to the theory of atmospheric refraction, *Bulletin Geodesique*, 107, 13-34.
- Steigenberger, P., M. Rothacher, R. Dietrich, M. Fritsche, A. Rüike, and S. Vey (2006), Reprocessing of a global GPS network, *Journal of Geophysical Research*, 111, B05402, doi:10.1029/2005JG003747.
- Tesmer, V., and H. Kutterer (2004), An advanced stochastic model for VLBI observations and its application to VLBI data analysis, in *International VLBI Service for Geodesy and Astrometry 2004 General Meeting Proceedings*, edited by N. Vandenberg and K. Bayer, pp. 296-300, NASA/CP-2004-212255, NASA, Greenbelt.
- Tesmer, V., H. Kutterer, and H. Drewes (2004), Simultaneous estimation of a TRF, the EOP and a CRF, in *International VLBI Service for Geodesy and Astrometry 2004 General Meeting Proceedings*, edited by N. Vandenberg and K. Bayer, pp. 311-314, NASA/CP-2004-212255, NASA, Greenbelt.
- Titov, O., V. Tesmer, and J. Boehm (2004), Occam v6.0 software for VLBI data analysis, in *International VLBI Service for Geodesy and Astrometry 2004 General Meeting Proceedings*, edited by N. R. Vandenberg and K. Bayer, pp. 267-271, NASA/CP-2004-212255, NASA, Greenbelt.